A Spectroscopic Analysis of the Main Sequence A star, KIC 11145123

Masahide Takada-Hidai (Tokai University)
D. Kurtz (Univ. Central Lancashire)
H. Shibahashi (Univ. Tokyo)
S. Murphy (Univ. Sydney, Arhus Univ.)
M. Takata (Univ. Tokyo), H. Saio (Tohoku Univ.)
T. Sekii (Univ. Tokyo)

Contents

0.　星震学（asteroseismology) の基礎

・地震波の伝搬の観測　→　地球内部構造の探査

・太陽・恒星の振動の観測　→　太陽・恒星内部構造探査

・解析法：　振動の速度場 → 球面調和関数　Y_l^m　(θ, ϕ）で展開。

固有振動数(ωnlm)の指数：

n … radial node number (動径方向の固有関数のゼロ点数）
l … angular order number　（角次数，球面上の固有関数ゼロの節線総数）
m … azimuthal order number（子午線に平行な節線数）　$-l \sim +l$ までとれる。

・**基本振動　n = 0，倍振動（overtone)　n ≠ 0**

・ある　n, l に対して、**球対称**での振動数はm に依存しないので、同じ振動数かつ異なる変位パターンのsingletが$2l+1$ 個縮退して振動モードを作るため、そのパワースペクトルのピークは**multiplet** になっている。　→　球対称が回転（Coriolis force ）や媒質分布変化（移流 advection) などにより破綻すると、縮退が解けて、個々のsinglet が少しずつ異なる振動数を持つ。→　**splitting**　が起こる。→　**回転などの情報が得られる。**

・radial mode …. $l = 0$ mode で表面に節線なし。動径方向に振動。

・$l > 0, m = 0$ …..　赤道面に平行な節線による帯状の振動。

・$l > 0, m \neq 0$ ….　緯度に沿うl-m本の節線とm本の子午線に沿う節線によりモザイク状振動。

自転による地震波正規モードのsplitting 例:　$_nS_l$

(上図）
低緯度観測点

（下図）
極近傍観測点

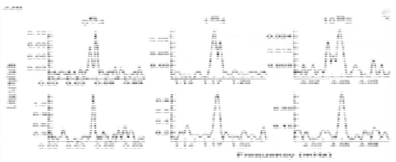

球面調和関数の例：　P_l^m $(\cos\theta)$=**Legendre 陪関数**

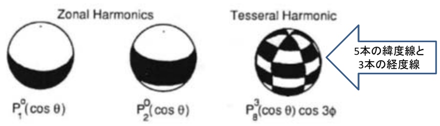

恒星における固有振動モード

p　モード（音波モード、pressure mode），　復元力＝圧力　. . . 高振動数の波動
g　モード（重力波モード、gravity mode），　復元力＝浮力　. . . 低振動数の波動
f　モード（表面重力波モード、fundamental mode),　復元力＝浮力

・n = 0 → f　モード　　　**・n ≠ 0 → p、g　モード**

・l = 0 →　動径モード　→　浮力なし　→　pモードのみ。

・pモードの伝搬：　音速　$\propto \sqrt{p/\rho}$　$\propto \sqrt{T/M}$ →　内部で**反射・屈折（スネルの法則）**

自転なし（球対称）

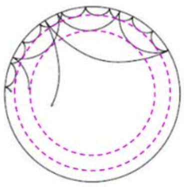

自転あり→振動数の変化→　splitting！

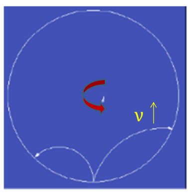

・モードの伝播領域：　太陽の例　（ⓒ『太陽』--現代天文学シリーズ--）

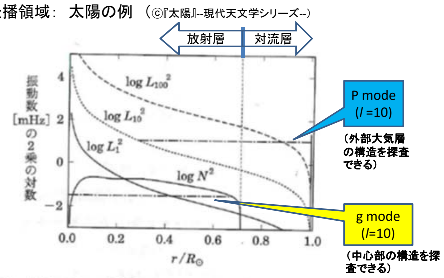

図 3.3　太陽モデルの伝播図．ラム振動数 ($l = 1, 10, 100$) とブラントーヴァイサラ振動数の分布を示している．一点鎖線は $l = 10$ の場合の伝播域の例を，p モードの振動数帯からひとつ (上)，g モードの振動数帯からひとつ (下) 示したもの．縦の破線は放射層と対流層との境界を示す．

1. Introduction and Purposes

- Kurtz+(2014, MNRAS, 444, 102) found that a main-sequence A star KIC11145123（Our target) shows both δ Sct p-mode and γ Dor g-mode pulsations.

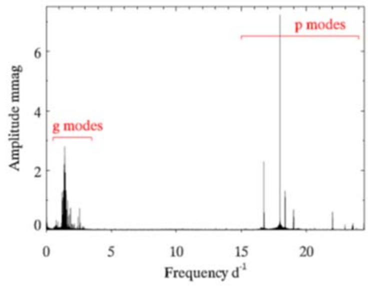

g mode triplets

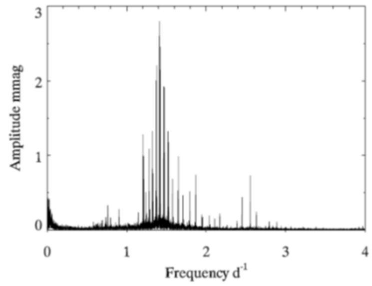

p-mode

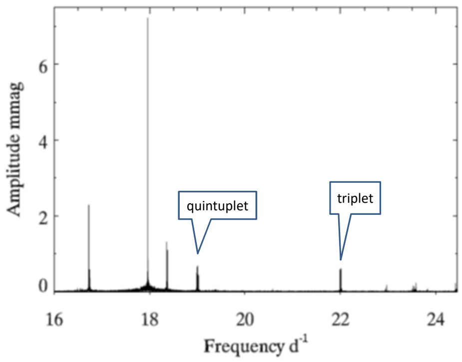

p-mode triplet and quintuplet

Diploe mode (l=1)　　Quadrupole mode (l=2)

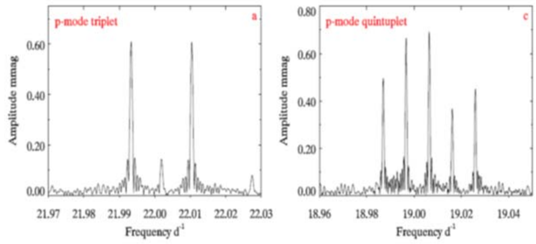

- Kurtz+(2014, MNRAS, 444, 102) argued that:

→ The robust determination of the **rotation of the deep core and surface** of the star. Period of rotaion ratio: ***P*(core) : *P*(surface) = 1 : 0.93**

→ Its rotation is the **nearly rigid rotation with a period near 100 days**, so that it is very important to clarify **what a strong angular momentum transfer mechanism** operates to make a rigid slow rotation.

- Among A stars, there are slow rotators such as magnetic Ap stars and non-magnetic Am stars.

→ No known Ap star shows such low overtone p modes and g modes as detected in KIC 11145123.

→ Am stars are generally slow rotator.

→ Our target may be **Am star or not**?

- Blue straggler stars are known to show slow rotation (Vsin *i*) with mostly less than a few 10 km/s.

→ Our target may be **blue straggler star or not**?

Purposes:

To clarify the properties of our target, we carried out the spectroscopic analyses, based on the high-dispersion spectra observed with HDS on the Subaru telescope.

Issues to be clarified:

1. Atmospheric parameters: Teff, log *g*, ξ, [Fe/H]
2. Radial velocity: Vrad → stellar population
3. Rotation velocity: Vsin *i* → asteroseismic Vsin *i* correct?
   what local velocity fields?
4. Abundances: [X/H], [X/Fe] → how are pattern and trend ?
   Am or Blue straggler ?
   what stellar population ?
5. Magnetic field: → try to search for <H>

2. Observations and Reduction

2.1 Observations

- KIC 11145123 basic data:
  α=19:41:25.3, δ= +48:45:15.08
  Kp=13.123, *J*=12.441, *H*=12.356, *K*=12.335
- Observation Date: 2015 July 3
- Subaru HDS (Echelle spectrograph)
- StdYc setup with wavelength range:
  Blue part: 4400—5720 A, Red part: 5800 — 7120 A
- Image Slicer #3 was used.
  → Wavelength resolution = 160000
- Total exposure time = 8000 sec (4 exposures)

2.2 Reduction

IRAF-Echelle package is used for standard procedure of CCD data reduction:

- bias, background, and cosmic ray subtraction
- flat-fielding
- extraction of single spectra
- dispersion correction for wavelength scale
- coaddition and combination of spectra
- normalization of spectra
- Doppler correction: 64 Fe I and 24 Fe II lines are used to obtain radial velocity Vrad.
  → apparent Vrad = -145.38 ±0.21 km/s
  → heliocentric V_h = -135.35 ±0.21 km/s

- Wavelength resolution R = 160000
  Th-Ar comparison spectra are measured to obtain FWHM and core intensity from which R is estimated.
- Signal-to-Noise (S/N) ratios:
  photon counts of continua at central wavelength of each orders are measured to obtain S/N ratios.
  80 – 120 and average 107 in blue region,
  100 – 120 and average 112 in red region,
  → S/N of the spectra is ~100 – 110.

3. Analyses of Atmospheric Parameters

Atmospheric parameters : Teff, log *g*, ξ, [Fe/H]

- Estimated following the method of Takeda + (2002, PASJ, 54, 451), based on the equivalent widths of selected Fe I and Fe II lines.
- The basic principle of the method:
  → to find the solution in the (Teff, log *g*, ξ) space, iterating the model from the starting model by changing values of each parameters.

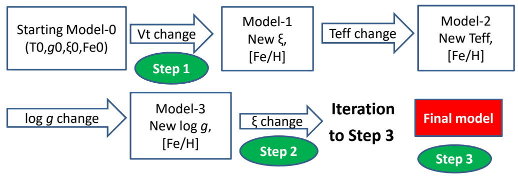

3.1 Model and line data

- SPTOOL code (Takeda, 2006) : for sp. synthesis, abundance.
  The code is based on Kurucz ATLAS9 and WIDTH9 codes.
- Model: 1D LTE model of Kurucz (1993) ATLAS9
- *gf* values: 67 Fe I lines … Westin+ (2000, ApJ,530,783)
  21 Fe II lines … Westin+ (2000) for 15 lines,
  Takeda+ (2005, PASJ,57,27) for 6 lines.

3.2 Step 1

(1) ξ (microturbulence)

- Starting model:Huber+(2014, ApJS, 211, 2)
  Teff= 8051 K, log *g*= 3.97, [Fe/H]= - 0.14
- Teff, log *g* = fixed,
- Requirement: Fe I abundances are independent on equivalent widths (W_λ).
  |(Wmax – Wmin) x a1| < σ(FeI) (Takeda+, 2002) …. (A)
  where Wmax=$W_{\lambda,max}$, Wmin=$W_{\lambda,min}$, a1 = slope of linear fit to log FeI vs W, and σ(FeI)= one standard deviation of log Fe I.
- The iterations are repeated in Step 2 and 3 to obtain the final ξ, which satisfies (A).

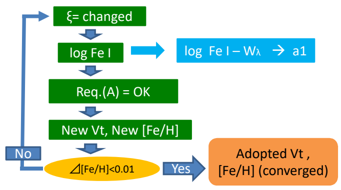

3.2 Step 1

(2) Teff (Effective temperature)

- Starting model: Teff = 8051 K, log *g* = 3.97, ξ = 2.87, [Fe/H] = -0.42
- log *g*, ξ = fixed.
- Requirement: Fe I abundances are independent on lower excitation potential (χ).

  |⊿χ x a1| < σ(FeI) , (Takeda+, 2002) .... (B)

  where ⊿χ is a deference of maximum and minimum of χ, and a1 is the slope of linear fit to log Fe I – χ trend.

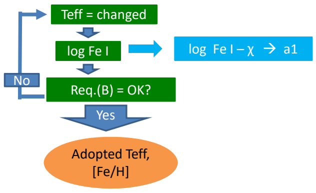

3.2 Step 1

(3) log *g* (Gravity)

- Starting model:

  Teff = 7585 K, log *g* = 3.97, ξ = 2.87, [Fe/H] = -0.63
- Teff, ξ= fixed
- Requirement: Fe I and Fe II abundances are equal.

  |<log FeI> - <log FeII>| < ε(FeI) + ε(FeII), (Takeda+2002) ... (C)

  where probable error ε ≡ σ/SQRT(N) for log FeI and log FeII, and <log FeI> and <log FeII> are average abundances. N is a number of lines.

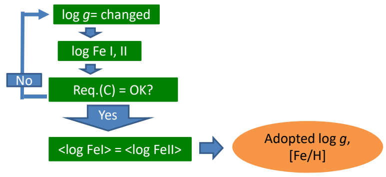

3.3 Step 2 and Step 3 for Final Model

- Resulting model in Step 1 = starting model.

  Teff = 7585 K, log *g* =4.19, ξ = 3.05 km/s, [Fe/H] = -0.72
- Requirements for Teff, log g, and Vt should satisfy;

  |(Wmax – Wmin) x a1| < σ(FeI) for ξ, (A)

  |⊿χ x a1| < σ(FeI) for Teff, (B)

  |<log FeI> - <log FeII>| < ε(FeI) + ε(FeII) for log *g*, (C)

  to obtain converged parameters.

Step 2

- Converged ξ = 3.08 km/s
- Converged Teff: requirement (B) → 7614 K

  requirement (C) → 7564 K

  Both Teff satisfy both (B) and (C) → average Teff = 7590 K adopted.
- Converged log *g* = 4.22
- Converged [Fe/H] = -0.71

-Resulting model in Step 2:

Teff = 7590 K, log *g* = 4.22, ξ= 3.08 km/s, [Fe/H] = -0.71

Step 3

- Confirm whether parameters satisfy requirements (A) – (C).
- ξ: see Fig.1 and 2. → confirmed → 3.08 +0.57, -0.40 km/s
- Teff: see Fig. 3 and 4 → confirmed → 7590 +82, -135 K
- log *g*: see Fig. 5 and 6 → confirmed → 4.22 ±0.13
- [Fe/H]: log FeI and log FeII → average log Fe → -0.71 ±0.11

< Final model >

Teff = 7590 + 82, - 135 K

log *g* = 4.22±0.13

ξ = 3.08 +0.56, - 0.40 km/s

[Fe/H] = -0.71 ±0.11

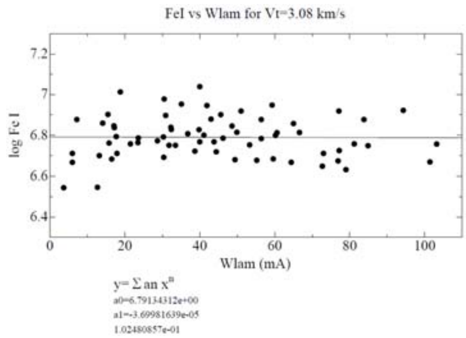

Fig. 1. log Fe I vs Equivalent widths for ξ=3.08 km/s.

⊿Wλ = 99.5 mA a1 = - 3.69981639E-05 σ = 0.104~0.110

|⊿Wλ x a1|=0.0368 < σ is satisfied.

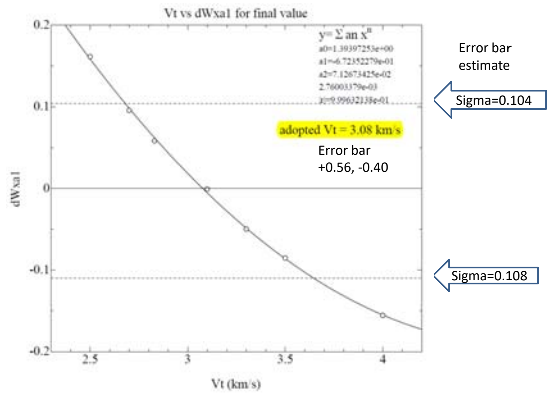

Fig. 2. Requirement (A) for ξ=3.08 km/s.

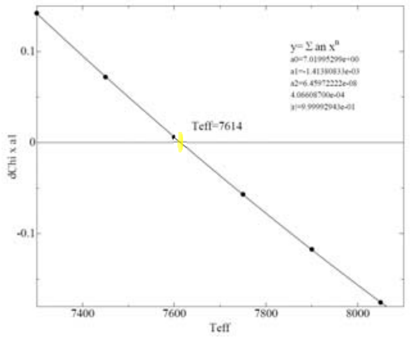

Fig. 3. Teff determination from Req.(B) :Teff vs ⊿χ･a1.

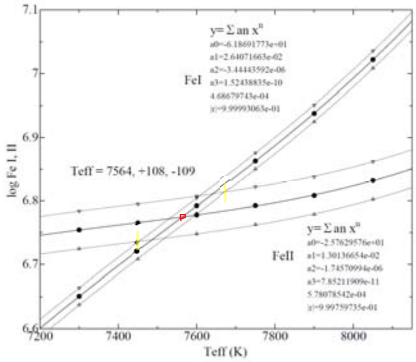

Fig. 4. Teff determination in Step 2 from Req. (C)

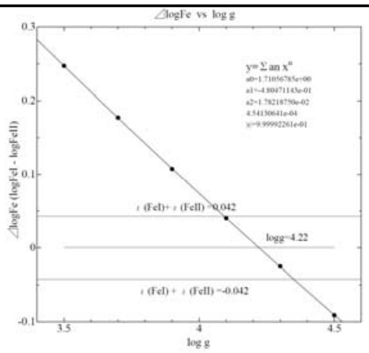

Fig. 5. log *g* determination from Req.(C).
<log Fe I> =<log Fe II> should be held.

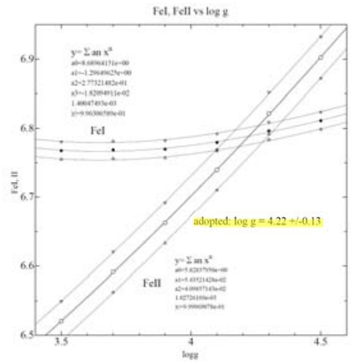

Fig. 6. log *g* determination from Req. (C).
<log Fe I> =<log Fe II> should be held.

4. Analysis of Rotation Velocity

4.1 Data used for the analysis:

1) Clean Fe I and II lines selected from the lines used for determination of atmospheric parameters.
   → 51 lines of Fe I, 19 lines of Fe II are used.
2) Lines used in Landstreet et al (2009, A&A, 503, 973): CrII 4634.0 A, FeI 4637.5 A and CrII 4554.9 A, TiII 4563.7 A. → These lines are used to confirm the Landstreet et al's argument.
3) Th-Ar emission spectra for determination of spectral resolution (R) and instrumental profile.

4.2 Method

1) The program MPFIT in the code SPTOOL (Takeda, 2006)
   → to derive a total broadening velocity (V_T) by fitting Gaussian profiles to observed ones （Takeda et al 2008）.
   Definition: $V_T^2 \equiv V_r^2 + V_m^2 + V_i^2$; $V_{r+m}^2 \equiv V_r^2 + V_m^2$.
2) ξ=3.08 km/s and the instrumental profile with $V_i = C_0/2R\sqrt{\ln 2}$ = 1.126 km/s corresponding to R= 160000 , C_0 光速度.
3) A broadening velocity V_{r+m} = convolution of rotation (V_r) and macroturbulence (V_m) = $\sqrt{V_T^2 - V_i^2}$.
4) V_M are estimated for lines of Landstreet et al. to confirm their argument.
5) Fe I and Fe II give V_T values to obtain the final V_{r+m}.

Results:

1. Confirmation of results of Landstreet et al (2009)

Landstreet+ (2009) argued:

Vsin*i* is dependent on line strength; Vsin*i* ∝ W_λ, so that the signatures of local velocity field may become more evident in stronger lines.

Table 1 shows our results of V_T and Vr+m (km/s).

Tab.1

line	W_λ (mA)	V_T	Vr+m
Cr II 4554	33.0	6.69	6.59
Cr II 4634	42.0	6.75	6.66
Ti II 4563	174.2	7.54	7.45
Fe I 4637	17.8	6.00	5.89

- Vr+m (Vsin*i*) is confirmed to depend on W_λ.

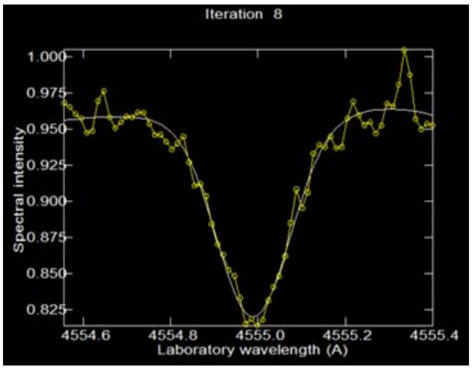

Fig. 7. Gaussian fitting to Cr II 4554 line.

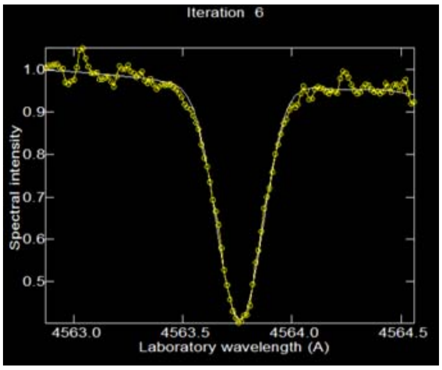

Fig.8. Gaussian fitting to Ti II 4563 line.

2. Fe I and II lines

V_M and Vr+m are analyzed for both Fe I and Fe II lines.

Fig. 9: Correlation of Vr+m with W_λ for Fe I lines.

Fig. 10: Correlation of Vr+m with W_λ for Fe II lines.

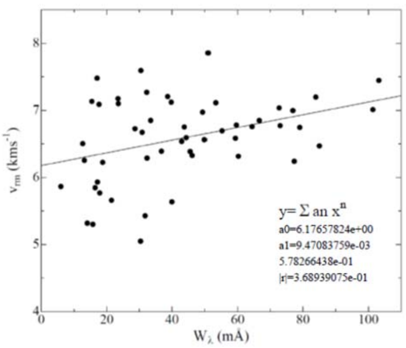

Fig. 9. Correlation of Vr+m with Wλ. for Fe I lines.

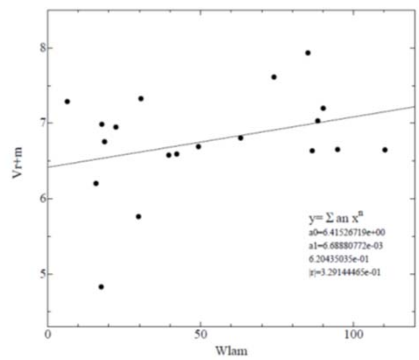

Fig. 10. Correlation of Vr+m with Wλ for Fe II lines.

Results:

As seen from Fig. 9 and 10, Vr+m of Fe I lines distributes with smaller deviation than that of Fe II lines.

→ Adopte Vr+m of Fe I lines.

- As discussed by Landstreet+ (2009), the true value of vsin*i* is (at most) as large as the minimum value found using the weakest, sharpest lines, implying that the influence or effect of local velocity field becomes minimum at the limit of W_λ = 0 mA.
- Fig. 9 gives the intercept of $V_{r+m,0}$ = 6.18 km/s, and regarded as *apparent* rotation velocity Vsin*i*, because we cannot separate rotation component (true Vsin*i*) from $V_{r+m,0}$.

Adopted apparent projected rotation:

Va sin*i* = 6.2 ± 0.6 km/s

- **Problem**: If Vsin*i* = 1 km/s inferred from asteroseismology is true, what local velocity field is responsible for apparent Vsin*i* ?

5. Abundance Analyses

5.1 Atomic data

- gf values for elements except for Fe I and Fe II:
  Kurucz & Bell (1995, CD-ROM#23) updated by
  Castelli & Hubrig (2004, A&A, 425, 263).
- Hyper fine splitting (hfs):
  Ba II …. McWilliam (1998, AJ, 115, 1640)
  Isotopic ratio is also adopted.
  → abundance diff. = 0.0 -- 0.3 dex
  Other Elements …. Kurucz (2011, website)
  Sc II, Mn I … lines stronger than 20 mA are treated with hfs effect.
  → abundance diff. < 0.1 dex

5.2 Measurements and calculations

(1) Measurements:

Equivalent widths (W_λ) are measured with Gaussian profile fitting for almost all lines by SPSHOW program in SPTOOL. Direct integrations are used for blended lines which are not fitted with Gaussian profile.

(2) Calculations:

- Abundance calculations are carried out by WIDTH program in SPTOOL, which is modified version of WIDTH9.
- Lines with hfs components are calculated by MPFIT program in SPTOOL to derive their abundances.

(3) Error estimations:

- Errors due to measurements of W_λ, gf-values
  → standard deviation (σ) of average abundances of each ions.
- Errors due to uncertainties of atmospheric parameters:
  ΔTeff = +82, - 135 K; Δlog *g* = ± 0.13;
  Δξ = + 0.57, - 0.40 km/s.
  → $\sigma_{tg\xi} = \sqrt{\sigma_t\text{^}2 + \sigma_g\text{^}2 + \sigma_\xi\text{^}2}$
- Total errors $\sigma_{tot} = \sqrt{\sigma\text{^}2 + \sigma_{tg\xi}\text{^}2}$

5.3 Results

(1) Table 2 demonstrates the abundances of each ions.

Tab.2. Abundances of each ions on the scale of log H=12. The solar abundances are taken from Asplund et al. (2009).

Code	Ion	log X average	[X/H]	[X/Fe]	Std.Dev. 1 σ	Error tgξ	Total error	No. of lines	Remark	Sun
3.00	Li I	< 1.38	< 0.33	< 1.04	···	···	···	1	1 doublet	1.05
6.00	C I	7.82	-0.61	0.10	0.15	0.05	0.16	10	2 doublets	8.43
8.00	O I	8.38	-0.31	0.40	0.09	0.09	0.13	3	3 triplets	8.69
11.00	Na I	5.75	-0.49	0.22	0.04	0.04	0.06	4	1 doublet	6.24
12.00	Mg I	7.13	-0.47	0.24	0.04	0.06	0.07	3		7.60
12.01	Mg II	7.29	-0.31	0.40	···	0.11	0.11	1	1 triplet	7.60
14.00	Si I	7.05	-0.46	0.25	0.22	0.04	0.22	14		7.51
14.01	Si II	7.03	-0.48	0.23	0.07	0.08	0.11	3		7.51
16.00	S I	6.87	-0.25	0.46	0.08	0.03	0.09	8	1 doubet,3 triplet	7.12
20.00	Ca I	5.95	-0.39	0.32	0.12	0.07	0.14	25		6.34
20.01	Ca II	6.02	-0.32	0.39	0.09	0.06	0.11	3		6.34
21.01	Sc II	2.80	-0.35	0.36	0.15	0.06	0.16	9	4 hfs fit	3.15
22.00	Ti I	4.59	-0.36	0.35	0.11	0.06	0.13	15		4.95
22.01	Ti II	4.59	-0.36	0.35	0.18	0.06	0.19	32		4.95
24.00	Cr I	4.90	-0.74	-0.03	0.11	0.07	0.13	14		5.64
24.01	Cr II	4.96	-0.68	0.03	0.12	0.05	0.13	21		5.64
25.00	Mn I	4.57	-0.86	-0.15	0.05	0.06	0.08	7	2 hfs fit	5.43
26.00	Fe I	6.79	-0.71	0.00	0.10	0.08	0.13	67		7.50
26.01	Fe II	6.79	-0.71	0.00	0.14	0.08	0.16	21		7.50
28.00	Ni I	5.70	-0.52	0.19	0.10	0.06	0.12	41		6.22
29.00	Cu I	3.56	-0.63	0.08	0.05	0.07	0.09	2	uncertain	4.19
30.00	Zn I	4.15	-0.41	0.30	0.03	0.06	0.07	3		4.56
39.01	Y II	1.87	-0.34	0.37	0.06	0.07	0.09	7		2.21
40.01	Zr II	2.38	-0.20	0.51	···	0.06	0.06	1	uncertain	2.58
56.01	Ba II	1.58	-0.60	0.11	0.04	0.15	0.15	4	4 hfs fit	2.18
58.01	Ce II	1.26	-0.32	0.39	···	0.08	0.08	1	uncertain	1.58
60.01	Nd II	0.91	-0.51	0.21	···	0.09	0.09	1	uncertain	1.41

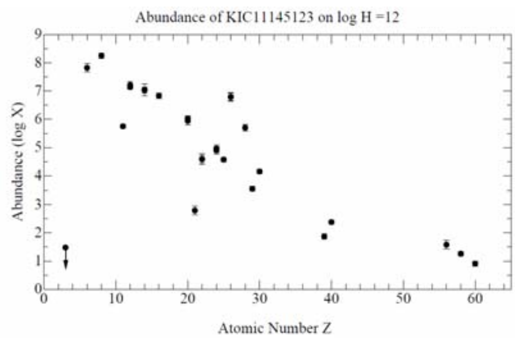

(2) Abundance pattern of [X/H] vs atomic number Z.

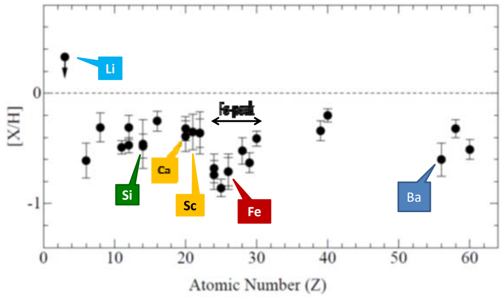

Fig.11 Abundance pattern of [X/H] with Z.

(3) Abundance pattern of [X/Fe] vs Z.

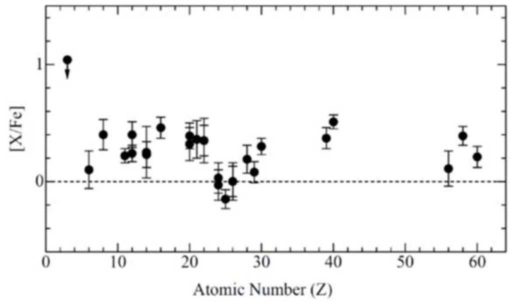

Fig. 12 Abundance pattern of [X/Fe] vs Z.

(4) Comparison with normal A, Am, and Ap stars.

(A) Comparison with normal and Am stars.

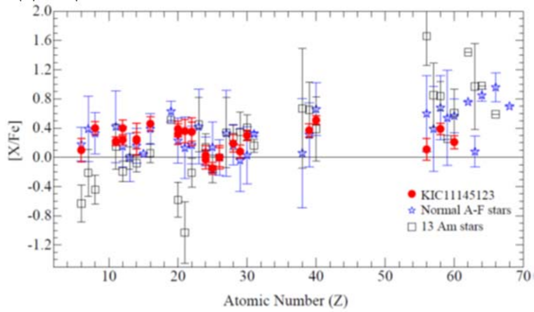

Fig. 13. Normal A-F stars and 13Am stars: Niemczura+(2015).

(B) Comparison with normal and (ro)Ap stars.

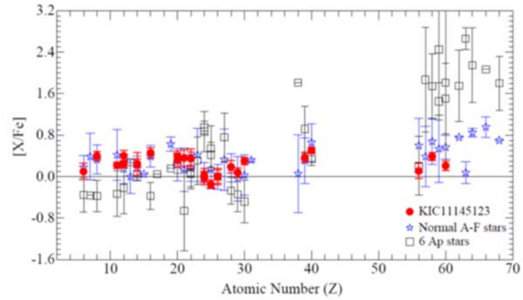

Fig. 14. Abundance pattern of our target, normal A-F stars, and 6 Ap stars (HD203932, 10 Aql, bet CrB, 33 Lib, KIC4768731, and HD41641).

(C) Comparison with δ Sct stars.

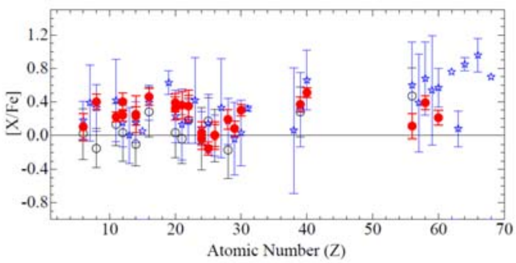

Fig. 15. Filled circle:KIC11145123, star: normal stars(Niemczura+2015), open circle: δ Sct stars (Fossati+2008).

(D) Comparison with γ Dor stars.

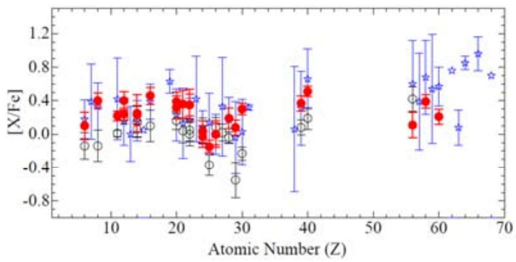

Fig. 16 Comparison of KIC11145123 with normal and γ Dor stars. Filled circle:KIC11145123, star: normal stars(Niemczura+2015), open circle: γ Dor stars (Bruntt+2008).

(5) Comparison with Blue Straggler Stars.

(A) Comparison of [Li/Fe].

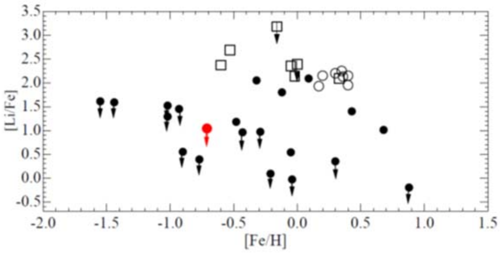

Fig.17

Fig16-Abundance pattern of [Li/Fe] vs [Fe/H]. Black dot: Glaspey+(1994) high velocity A-F stars and blue stragglers; Red dot: KIC 11145123. Normal A stars from Takeda+2012 (open square) and Burkhart2000 (open circle).

(B) Comparison of [C/Fe] and [O/Fe].

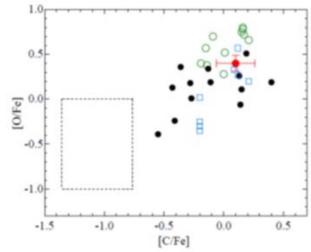

Fig.18 [C/Fe] and [O/Fe] ratios of blue stragglers in NGC6752 (black filled circle:Lovisi+2014) and M4 (green open circle:Lovisi+2010), and TO dwarf stars in NGC6752 (blue open square: Carretta+2005) and our target, KIC11145123 (red filled circle). CO-depleted blue stragglers in Ferraro+2006 distribute in the box with dashed line.

5.4 Summary of Abundances of KIC 11145123

1. No under-abundances of [Sc/Fe] and [Ca/Fe] → not Am star.
2. No over-abundance of [Cr/Fe] → not Ap star.
3. General pattern is more consistent with normal A stars rather than Am and Ap stars.
4. General pattern is consistent with both δ Sct stars and γ Dor stars due to the same average difference from KIC values.
5. Abundance trends of [Li/Fe], [C/Fe], and [O/Fe] are consistent with blue straggler stars. C and O are not depleted.

6. Magnetic field

Mathys (1990) method: Fe II 6147.7, 6149.2 A line ratio.

→ magnetic field modulus <H>

$\triangle W = W(6147.7) - W(6149.2)$

$\overline{W} = [W(6147.7) + W(6149.2)]/2$

→ $\triangle W/\overline{W} = 0.087$

→ $\langle H \rangle = 2.7 \pm 0.4$ kG from Mathys & Lanz (1992) 's empirical relationship.

Fig. 19 depicts observed and synthetic spectra of Fe II lines.

→ Asymmery of line core of Fe II 6149.2 line is not confirmed due to low quality and line broadening.

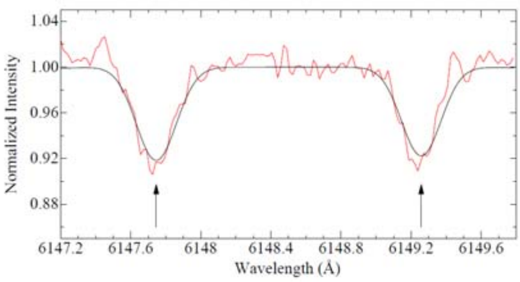

Fig. 19 Observed Fe II 6147.7 and 6149.2 A lines (red) and the synthetic spectrum (black) which is computed with Va sin*i* = 6.2 km/s.

7. Summary and discussion

1. Atmospheric parameters of Final Model
   Teff = 7590 + 82, - 135 K; log g = 4.22±0.13;
   ξ= 3.08 +0.57, - 0.40 km/s; [Fe/H] = -0.71 ±0.11;
   heliocentric radial velocity Vh = -135.35 ±0.21 km/s.
   - [Fe/H] and Vh may suggest that KIC 11145123 is a metal-poor thick disk star of Pop. II. → How is age ?
   - ξ ~ 3km/s is consistent with those of Am stars (Landstreet+ 2009) and also with those of blue straggler stars(Glaspey+ 1994).

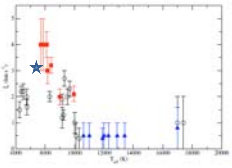

Star: KIC11145123
Red square: Am stars.
Open circle: normal stars.
Triangle: HgMn stars.

2. Rotation Velocity (Vsin*i*)

- $V_{r+m,0}$ = 6.2 ± 0.6 km/s is convolution of rotation velocity and macroturbulence, which are not separated in our calculation.

→ **adopted $V_{r+m,0}$ = *apparent* Va sin*i* = 6.2 ± 0.6 km/s**

→ Confirming the asterosesmic Vsin*i*.

- asteroseismology gives Vr = Vsin*i* = 1 km/s, and *i* ~ 70°

→ macroturbulence Vm = 6.5 km/s.

- **Problem:**

（1） What is velocity field responsible for Vm ?

→ Convection ? Pulsation ? Other mechanism ?

（2） What is mechanism responsible for the rigid rotation ?

3. Abundances

- Low metallicity [Fe/H] and high radial velocity suggest that KIC11145123 may be a thick-disk star or a blue straggler star.
- Population is not clear due to lack of distance and proper motion.
- Abundance pattern suggests that the star seems to be more consistent with a normal A star.
- Abundance pattern is consistent with both δ Sct and γ Dor stars.
- Abundance trends of Li, C, and O suggest that KIC11145123 is more likely a blue straggler star.

→ The values of [C/Fe] and [O/Fe] are normal.

→ This implies that the origin of KIC11145123 may be due to collision of two stars.

(If C and O are depleted, mass transfer/accretion origin.)

4. Magnetic field

<H> = 2.7 ± 0.4 kG is regarded as an upper limit.

If the magnetic field exists, it may contribute to make the star a slow rotator due to braking effect.

Thanks for your attention!